J Mater Sci (2009) 44:799–807
DOI 10.1007/s10853-008-3155-3

Modification of single-walled carbon nanotubes and its influence on the interfacial strength in polymeric composites

R. Mikael Larsen

Received: 5 November 2007 / Accepted: 2 December 2008 / Published online: 27 December 2008

Abstract Single-walled carbon nanotubes was purified and modified with dichlorocarbene, HNO_3 or octadecylamine and incorporated in polymeric matrices of polycarbonate and epoxy. Exposing the composite material to a tensile strain and measuring the shift of the G′-band revealed that higher loads could be transferred to the HNO_3-modified carbon nanotubes. Exfoliation was regarded as the main reason for the increased interfacial strength resulting in larger specific surface area and higher hydrostatic compressive stresses on the nanotube bundles.

Introduction

There are several reasons for incorporating carbon nanotubes in a polymeric matrix. One reason is the strengthening effect due to high stiffness, high aspect ratio, and small dimensions making them ideal for most manufacturing processes. Another possibility is to use the nanotube as strain sensors [1–3]. When the nanotube is subjected to mechanical deformation, many of the bands in the Raman spectrum move proportionally to the applied strain. With micro-Raman spectroscopy it is possible to measure the spectrum and thus the strain at spots down to 1 square micrometer. For the nanotube to work properly either as reinforcement or as a strain sensor it is very important that strain (or load) effectively can be transferred from the matrix to the nanotube. The interfacial strength between the matrix and the nanotube should be high. Carbon nanotubes with π-bonds on the surface are essentially a non-reacting material and form normally only weak bonds with other materials. Different ways have been suggested to modify or functionalize the nanotube mainly with the purpose to enhance the adhesive properties.

In this study, three different surface modifications of single-walled carbon nanotubes (SWCNT) are applied and were compared with a non-modified carbon nanotube material. The different SWCNT materials were embedded in a polycarbonate-matrix and an epoxy-matrix. The interfacial strength between the SWCNT and the matrix was evaluated by Raman spectroscopy measuring the peak position of the G′ band of the SWCNT as a function of the applied tensile strain. The G′ band ($\sim$2,600 cm^{-1}) is the second-order overtone of the D-band ($\sim$1,300 cm^{-1}) and is very sensitive to strain in the axial direction of the tube. The peak position shift is proportional to the applied strain [1–3].

The actual shift depends on the orientation of the nanotubes with respect to the load direction, orientation distribution, and the polarization geometry of the Raman microscope. Carbon nanotubes parallel to the load direction are ideally subjected to the same strain as the principal strain whereas carbon nanotubes perpendicular are subjected to opposite strain because of the contraction ratio or Poisson ratio.

In most cases, the nanotubes in composites are not unidirectionally aligned, but due to polarization it is still possible to measure strains in composites where the nanotubes have random directions. The intensity of the Raman bands is sensitive to the polarization of the laser beam. Hwang et al. found that the intensity of the RBM band is proportional to $\cos^4\theta$, where θ is the angle between the transmission axis and the nanotube [4]. On the other hand, Frogley et al. found that the intensity of G′ bands

R. M. Larsen (✉)
Department of Mechanical Engineering, Aalborg University, Pontoppidanstraede 101, 9220 Aalborg, Denmark
e-mail: rml@me.aau.dk

seems to fit $(\cos^2\theta - 0.5\sin^2\theta)^2$ [5]. In both cases, an analyzer with its polarization direction parallel to the incoming light was used. With either case using parallel polarization of the incident and scattered light, it is possible preferentially to measure the strain in carbon nanotubes with the same direction as the applied strain, and shift in the position of the G′ band was proportional to the strain.

The position of the G′-band is not only influenced by the tensile strain but also by the polymeric matrix. When embedding the SWCNT in a polymeric matrix, the G′ peak position moves from the normal $\sim$2,610 cm^{-1} in air to higher wave numbers. This is caused by several things. First, thermal stresses build up from the cooling from the glass transition temperatures. The thermal expansion coefficient of the matrix is considered to be larger than the coefficient of the SWCNT, thus the thermal contraction of the matrix is transmitted to, the nanotube via shear forces at the interface giving rise to axial compression of the nanotube [1]. Second, due to cohesive energy density, which is related to the surface energy of the matrix, large hydrostatic pressures are applied to the SWCNT. Chemical curing of epoxy will also lead to compressive stresses.

In this study, the interfacial strength is evaluated measuring the Raman shift of the G′-band. However, the laser spot size is large compared to the size of the nanotubes, and the shift will be an average from many individual nanotubes. Carbon nanotubes form bundles, and slip between individual nanotubes in the bundles can occur. In this case, the individual nanotubes may not have the same strain, and the measured shift will be an average from the individual nanotubes. Despite these objections, it is believed that measuring the shift versus strain is a useful way to evaluate the interfacial strength between the carbon nanotube and the polymeric matrix.

Modification

When talking about chemical modifications of CNT, a clear distinction between sidewall and end modifications should be made. In case of end modifications, the bonding mode of sp^2 does not change to a sp^3 mode. See Figs. 1 and 2. Instead, weak bonds in the tube, i.e., end caps and weak spots at the sidewall are broken and different groups are attached to the tube.

At sidewall modifications the π-bond has to be opened, and a change in bonding mode from sp^2 to sp^3 has to take place. The π-bond in the double bond in alkenes is not difficult to break, but the stability increases when going to the delocalized π-bond in aromatic rings and it stabilizes further when going to the π-bonds in graphite. Breaking double bonds in graphene sheets must lead to a rearrangement of the delocalized π-bonds probably resulting in a local weakening of the structure.

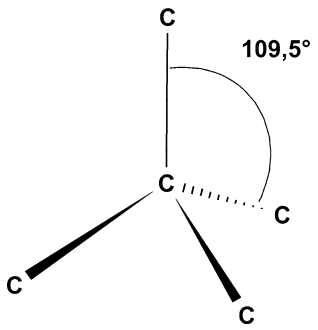

Fig. 1 The sp^3-hybridization. The carbon atom is bonded via single bonds to other carbon atoms. The structure is three-dimensional with 109.5° between the bonds

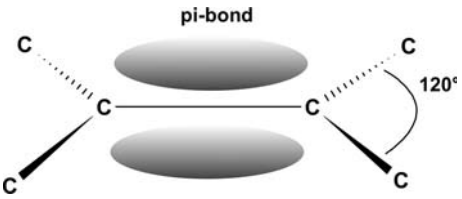

Fig. 2 The sp^2-hybridization. The carbon atom is bonded via a double bond to another carbon atom. The structure is flat with 120° between the bonds

In graphite, both the π-bond and the double bond are very strong. In carbon nanotubes, the bonds are stretched due to the curvature compared with graphite thus decreasing the bond strength. The stretching is higher at the end caps of the nanotubes due to the smaller radius of curvature and due to the presence of pentagons/heptagons leading to an angle between the bonds different from the equilibrium of 120°. Modification is thus more likely to take place at end caps of the nanotubes and SWCNT with small diameter compared to MWCNT with a large diameter. Chen et al. have a nice discussion on this topic in a paper from 1998 [6].

Modification involving dichlorocarbene

This is a modification using dichlorocarbene and is capable of attacking the double bond as shown in Fig. 3. Dichlorocarbene is an electrophilic reagent that helps to deactivate the carbon double bonds [6]. Normally, dichlorocarbene is made on site by reaction between chloroform and a strong aqueous solution of NaOH (see Fig. 4). In this case, the best results are achieved using phase-transfer catalyst like triethylbenzylammonium chloride.

Another possibility is to use potassium t-butoxide as the base in an organic solvent and adding chloroform dropwise.

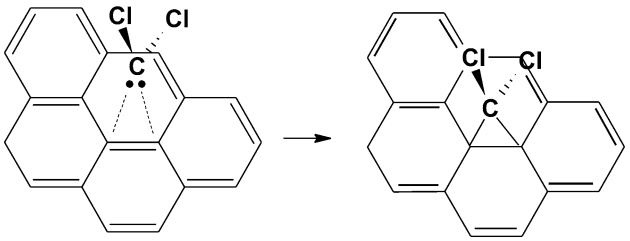

Fig. 3 Attack of a double bond in a graphene sheet by dichlorocarbene

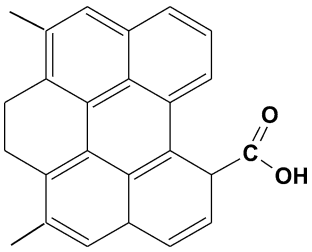

Fig. 5 Formation of carboxyl groups at free ends by treatment in HNO_3

Modification involving HNO_3

This modification involves treatment of the carbon nanotubes with concentrated HNO_3. Weak bonds especially at the ends are attacked and broken and an oxidation of the carbon is taking place forming carboxyl groups at the unbonded carbon (see Fig. 5). The carboxyl group is relatively reactive and other organic molecules can now easily be attached to the nanotube.

However, the HNO_3 probably also attacks weak spot on the tubes and will probably slowly oxidize all the carbon in the nanotubes. Especially, a mixture of concentrated H_2SO_4:HNO_3 in the ratio 3:1 is very aggressive and is used to cut nanotubes into smaller lengths [7].

Octadecylamine-modification

This method was adopted from the work of Chen et al. [8]. HNO_3-treated carbon nanotubes with carboxyl-groups are melted with stearylamine (octadecylamine). A proton-transfer is taking place and an ionic bond is established between the nanotube and the amine-group as shown in Fig. 6.

Experimental

Purification

In all modifications, purified SWCNT Grade AP from Carbolex was used. Purification is done by air annelaing at 275 °C followed by 5M HCl-reflux for 6 h. Suspension was filtered through a 0.45 μ PVDF-membrane filter and washed with deionized water until neutral pH. The purifications removed all amorphous carbon and some carbon particles and metal catalyst particles (Ni and Y). After the purification only ~20% of the initial material is left. Figure 7 shows the as-received and the purified CNT.

Modification by dichlorocarbene

Procedure

Purified SWCNT of 0.22 g was heated at 120 °C for 18 h in order to remove adsorbed water. The bottle was filled with Ar to prevent any adsorbsion of water. Sixty milliliters of tetrahydrofuran and 15 g of potassium-tetrabutylat were added. The mixture was placed on a NaCl-ice-water bath to keep the mixture cold. Chloroform ($CHCl_3$) of 8 mL was added dropwise. After the addition, the bottle was removed from the ice-water-bath and allowed to reach room temperature whereafter ice was added to the mixture to react with remaining potassium-tetrabutylat and to dissolve the precipitated potassium chloride. Next day, the mixture was shortly sonicated and was filtered through a 0.45 µm PVDF-membrane filter. The filtrate was washed with water and ethanol several times involving low-power ultra-sound and was dried at 100 °C for 18 h.

The weight increase was very close to 32%. If the weight increase only is caused by addition of dichlorocarbene, then the ratio between carbonatoms in the nanotube and attached dichlorocarbene is close to 22:1.

HNO_3 treatment

Procedure

Purified SWCNT of 0.50 g was refluxed in 50 mL 5M HNO_3 or 10M HNO_3 for 1 h.

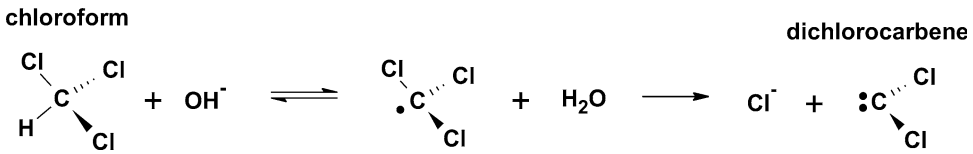

Fig. 4 Generation of dichlorocarbene by reaction of chloroform and a strong base

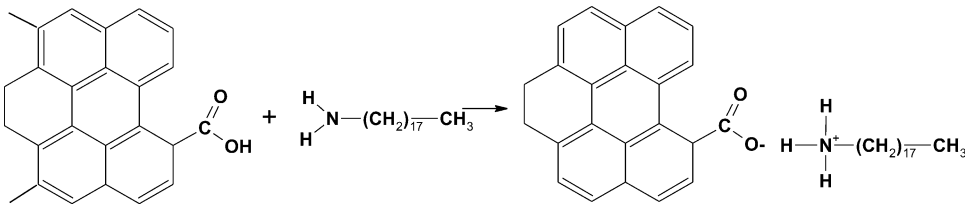

Fig. 6 Formation of an ionic bond between the carboxyl group on the nanotube and an amine

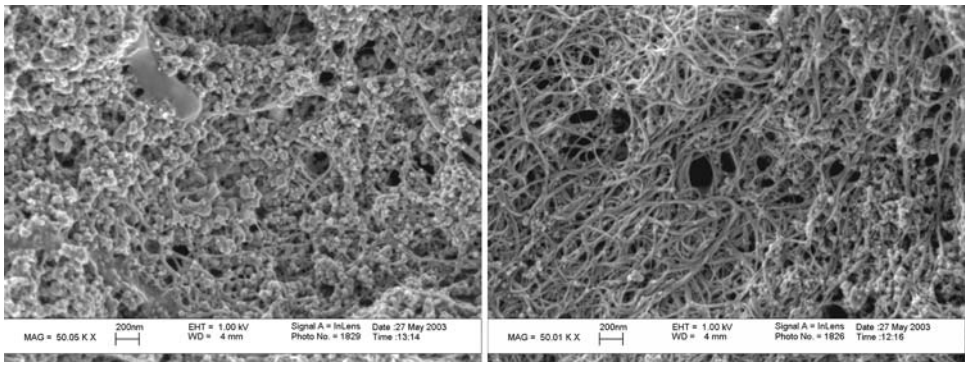

Fig. 7 SEM-pictures of as-produced (left) and purified (right) Carbolex AP. In the as-produced nanotube material, a lot of amorphous carbon is seen. In the purified sample, the amorphous carbon is absent, which was also confirmed by TGA-analysis. In the purified sample, nanoparticles together with nanotube bundles are seen

Octadecylamine-modification

Procedure

HNO_3-treated SWCNT of 0.23 g was placed in a beaker and heated to 100 °C for 18 h to get rid of absorbed water. Octadecylamine (stearylamine) of 2.01 g was added and the temperature was raised to 125 °C. At this temperature, the octadecylamine is melted and wetts the nanotubes. The mixture was left for 6 days whereafter 800 mL of ethanol was added to dissolve the remaining octadecylamine. This mixture was sonicated for 30 min and was filtered through 0.45 μm PVDF-membrane filter. It was necessary to keep the mixture warm to prevent the octadecylamine to precipitate before filtering. To be sure that all octadecylamine was removed, the filtrate was washed and sonicated in ethanol and filtered again two times. The filtrate was heated to 100 °C for drying.

In this case, the weight increase was 61% which corresponds to that every 34th carbon atom in the nanotube has been bonded to an amine group. This also means that not only the ends of the nanotubes are decorated with stearylamine, but the nitric acid also attacked weak spots on the sidewalls. The exact mechanism of this reaction and the influence on the mechanical properties of the nanotube is unknown. EDS-analysis was very difficult due to large amounts of adsorbed oxygen and nitrogen. However, an increase in the nitrogen content was observed.

Fabrication of composite material

Approximately 200 mg of carbonnanotube material was heated at 100 °C for at least 24 h to get rid of adsorbed water. In general the weightloss due to the heating was in the order of 10–15% indicating a high amount of adsorbed water. The amount of carbon nanotube material was adjusted to give a final content of 1 wt% of the original purified carbon nanotube material before the modification to enable the comparison of the mechanical properties.

Cyclohexanone of 60–80 mL was added and ultrasonically mixed with a 400 W dr. Heischel UP200s ultrasonic processor (cycle: 0.5; amplitude: 60%) for 2 h. Hereafter, 17–18 g of polycarbonate from Bayer (Tradename: Makrolon Grade M2405F) was added and stirred for several hours at 80–90 °C until PC was dissolved. Solution was left several days at room temperature. Furthermore the compound was heated in vacuum at 130 °C for 3 days in order to remove the cyclohexanone.

Injection moulding was carried out at 223 °C and the mould was heated to 75 °C.

For the epoxy composites, the carbon nanotubes was dispersed in 99.9% ethanol. The epoxy was mixed from 100 parts LM E20 and 35 parts LM H20; both are internal company names. LM E20 is a mixture of Bisphenol-A-diglycidylether with a mol-wt < 700 and minor amounts of Bisphenol-F-epichlorhydrin and 2.3-epoxy-propylneodecanoic. LM H20 is the hardener, which contains 3-aminomethyl-3,5,5-trimethyl-cyclohexylamine (IPDA), polyoxyalkylenamin, 2-methyl-1,5-pentandiamine, and benzylalcohol. LM E20 was added and the mixture was left at 60 °C until all ethanol was evaporated, and then the LM H20 hardener was added. Curing took place at 80 °C for 4 h. For the octadecylamine-modified carbon nanotubes, the dispersion of the carbon nanotubes was done in THF.

Raman spectroscopy

Raman spectra were obtained using a Renishaw Invia Raman microscope. The beam from a HeNe laser (632.8 nm) was focused through a 20X objective lens on the sample. To investigate the influence of strain on the shift of the G′ band ($\sim$2,700 cm^{-1}) small dogbone test bars were loaded in a small tensile test rig placed on the microscope table. The laser intensity was reduced and the spot was defocused to minimize local heating. Spot size was around 15 μm. The G′ peak was measured in back-scattered mode and VV sampling geometry, i.e., polarizer and analyzer parallel to load direction. The use of an analyzer increases the sensitivity as reported by Frogley et al. [5].

FTIR

Infrared spectroscopy was done with a in ATR mode. The samples were ultrasonically dispersed in iso-octane and the solution was placed on the ATR-crystal (ZnSe). Evacuation of the sample removed the iso-octane, and a good contact of the CNT-material on the crystal was obtained.

Results and discussion

FTIR

The FTIR spectra are shown in Fig. 8. The dichlorocarbene-modified CNT show only weak peaks. CH_2 stretching is seen at peaks around $\sim$2,900 cm^{-1}. XPS elemental analysis showed chlorine to be present in the sample; however, it is not possible to get any indication whether these results are from reaction products formed during the modifications or whether it really is the chlorine bonded covalently to the CNT.

For the HNO_3-modified carbon nanotubes the strongest peak is a broad peak around $\sim$1,700 cm^{-1} equivalent to C=O stretching. There is, however, not seen any peak for OH-stretching. The octadecylamine-modified CNT has a very different spectrum despite the inheritance from the HNO_3-modified CNT as shown in Fig. 9. A proton transfer occurs when the carboxylic acid combines with the amine group on the octadecylamine resulting in a carboxylate ion.

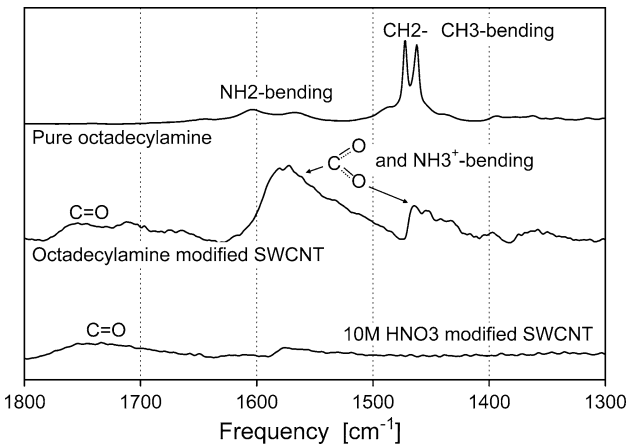

Fig. 9 Close-up of the FTIR spectra to show the difference between the HNO_3 and the octadecylamine modified carbon nanotubes

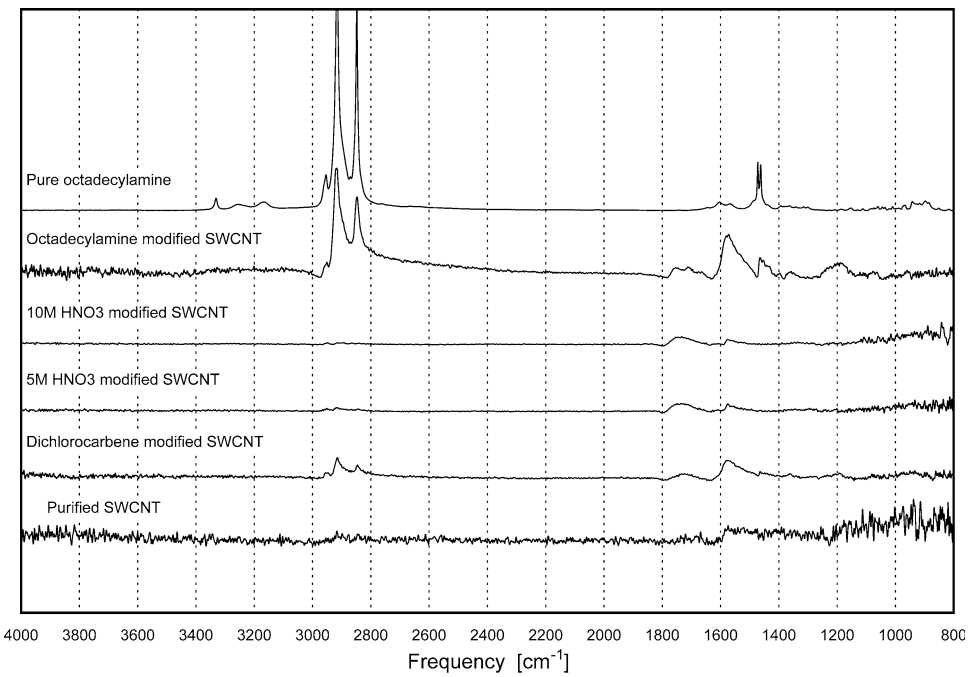

Fig. 8 FTIR spectra from the various carbon nanotubes materials

This is indicated by the appearance of two peaks at around 1,560 cm^{-1} and 1,450 cm^{-1} which are the asymmetric and symmetric stretching frequencies of the carboxylate ion [9], respectively. There is still some C=O stretching probably due to some carboxylic acid groups which did not bond to any amine group.

Raman shift

The Raman peak shift of the G′-band from the SWCNT as a function of the tensile strain is shown in Figs. 10 and 11. At small strains, there is a linear response of the peak shift versus strain with a negative slope hereafter also called the sensitivity. When the strain and thus the shear stress at the interface exceed the interfacial strength at the interface, the sensitivity fades and eventually the peak shift becomes constant. The epoxy itself had an elastic behavior up to a strain of at least 2% and polycarbonate up to 1.5%, so yielding of the polymeric matrices is not the cause for the breakdown of the interface.

In general, it is seen that the HNO_3-modified SWCNT has the highest sensitivity and the largest peak shift. In general, the sensitivity is larger for epoxy, i.e., 10–18 cm^{-1}/% strain compared to 4–8 cm^{-1}/% strain for the PC-composites. At zero strain, the G′ peak position is also generally higher for epoxy than for PC and it is also the largest for the HNO_3-modified SWCNT. Frogley, Wagner et al. have done experiments on different matrix materials with carbon nanotube and measured the response on the G′ peak position in tension [5, 10]. For epoxy matrix, the slope was ∼18 cm^{-1}/% strain, for polyurethane acrylate the slope was ∼6.3 cm^{-1}/% strain, and for an elastomer (RTV silicone rubber) with a low Young's modulus it was as low as 0.08 cm^{-1}/% strain. The reason for the low slope of the elastomer-composite was explained by a pseudo-yield of the elastomer giving rise to a loss of stress transfer at the interface. Measuring on isolated individual nanotubes, Cronin et al. found that the sensitivity was ∼37 cm^{-1}/% strain [11]. For highly aligned nanotubes in a PVA polymeric matrix, the sensitivity was found to be up to ∼40 cm^{-1}/% strain. In this study, the carbon nanotubes were isolated and not in bundles [12].

Several things can cause the large variation in the sensitivity. Here it is important to notice that we measure an average Raman shift and thus an average strain of individual SWCNT in the bundles, and also an average across the length of the individual nanotubes. For bundles the individual tubes can slide relatively to each other and thus the strain from the matrix may not be completely transferred to all the carbon nanotubes. And also the orientation of the carbon nanotubes in the matrix will have an effect on the sensitivity. Even for isolated carbon nanotubes the strain from the matrix will gradually be transferred to the tube from the ends as stated by the shear-lag model. This means that the average strain in the nanotube always is less than the strain in the matrix. The classic shear-lag model is based on continuum mechanics and does not necessarily apply on an atomic level, but the model can give an idea on how the strain is transferred [13, 14].

The shear stress can be evaluated from the strain profile by using the following equation, which can be derived from

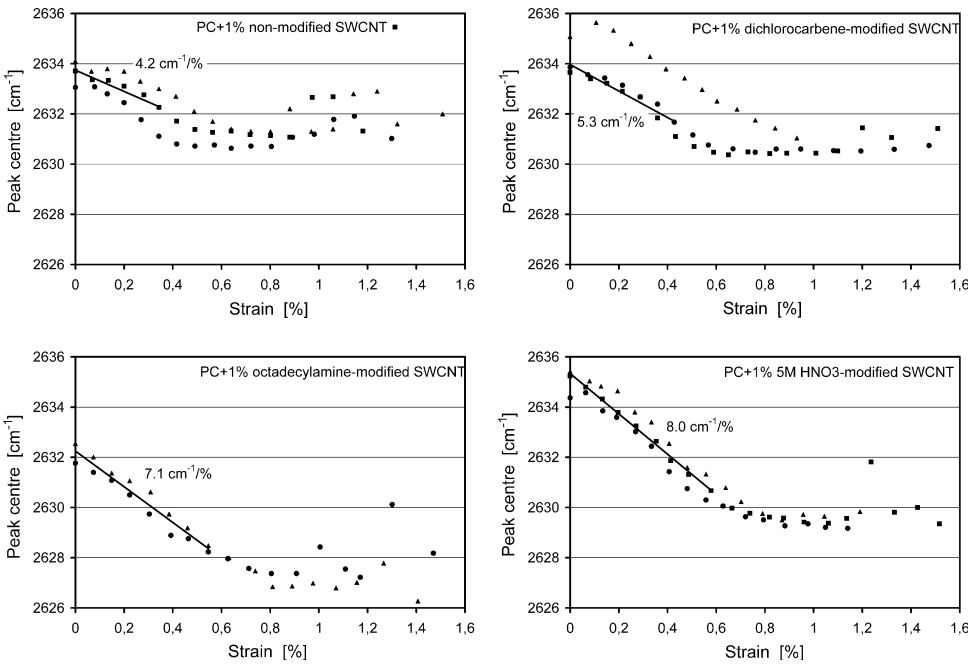

Fig. 10 Peak shift of the G′-band for the various PC-composite materials. Three sets of data have been used for the graph

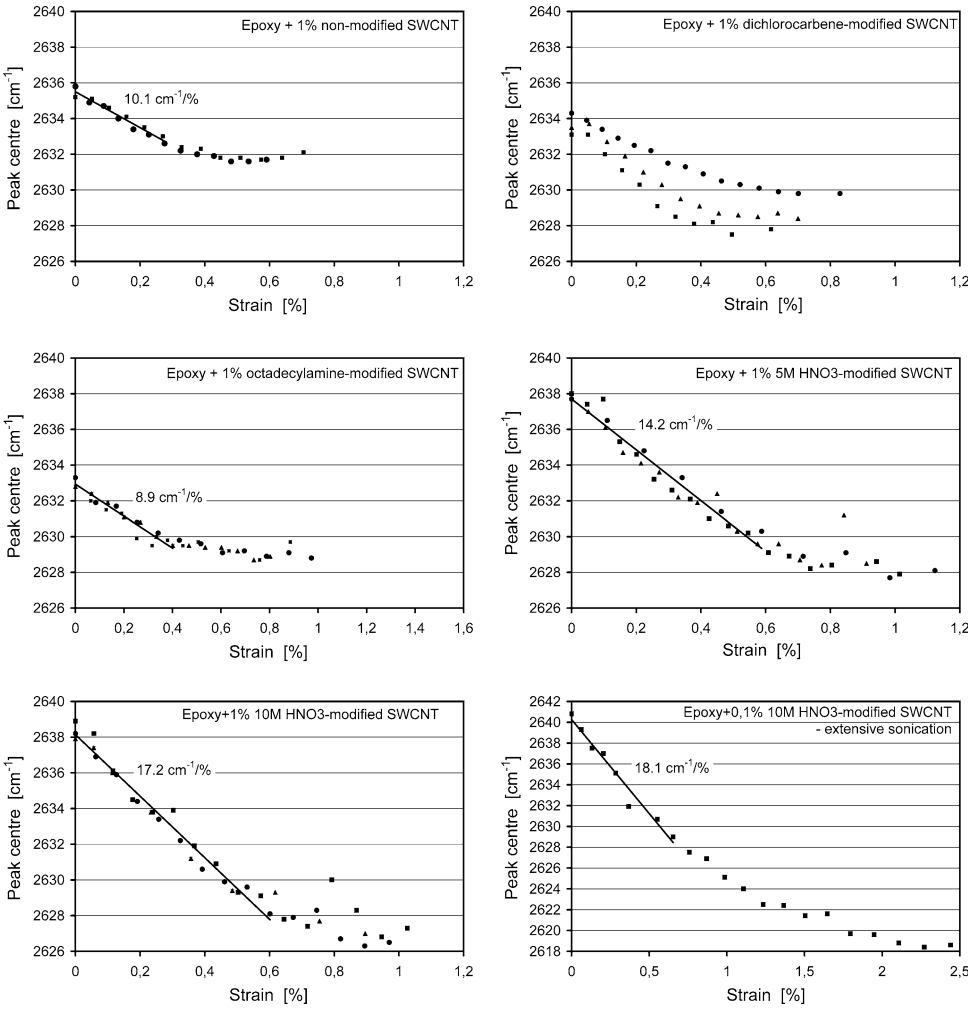

Fig. 11 Peak shift of the G′-band for the various epoxy-composite materials. Note the different scales of the axis in the epoxy + 0.1% 10M HNO_3-modified SWCNT. Three sets of data have been used for the graph except for epoxy added 0.1% 10M HNO_3-modified CNT, where only one set is used

a simple model where the shear forces at the surface and the tensile forces in the fiber are balanced [13].

$$\tau = \frac{E_f r}{2}\left(\frac{d\varepsilon}{dx}\right) \quad (1)$$

The shear stresses are the largest at the nanotube ends and are zero at the middle of the tube. Debonding will start at the fiber ends, but frictional forces will still transfer strain or stresses to the nanotube [13]. For a given maximum value of the shear interfacial strength, $d\varepsilon/dx$ increases with decreasing r and thus decreasing bundle size. This means that strain more quickly is transferred from the ends of the nanotube and the average strain will increase. This will cause an increase in the observed sensitivity.

Looking at the peak position at zero strain, it is interesting to see that it is high for nearly all samples with good strain transfer to the nanotubes, i.e., high sensitivity. The high peak position could be explained by higher compressive stresses from the matrix material. In this study, the peak position for as-received carbon nanotubes is around 2,610 cm^{-1}, whereas the peak positions for the embedded carbon nanotubes lie between 2,632 cm^{-1} and 2,641 cm^{-1} indicating high compressive stresses. Thermal contraction when cooling from the curing temperature or the glass transition temperature will cause compressive stresses as the thermal expansion coefficient is much larger for the polymeric matrix than for the carbon nanotubes [13, 15]. Chemical contraction when curing the epoxy will also give additional compressive stresses. However, compressive stresses can also arise from the hydrostatic pressure from the surrounding matrix caused by cohesive energy density. The size of this hydrostatic pressure is very large and depends on the cohesive energy density of the surrounding matrix. Wood et al. found that the peak position increases with the hydrostatic pressure whether it was a result of the cohesive energy density or of mechanically applied hydrostatic pressure [1, 2]. In this way, they were able to estimate the hydrostatic pressure which is in the order of 200–2,400 MPa.

The variation in the G′ band position at zero strain could be explained by variation in nanotube bundle size. In

smaller nanotube bundles a larger fraction of the nanotubes are in direct contact with the surrounding matrix. Axial stresses will mainly cause strain in the outer nanotubes in direct contact with the matrix material. The stress or strain distribution from the radial stresses within the bundles is unknown although it is possible that the outer nanotubes will again experience the highest strain. Thus smaller bundles will have a larger average compressive strain and thus a higher G′ band position and, again all other factors being equal, this position can be an indication on the bundle size and thus the distribution of the nanotubes. The solvation force or the cohesive energy density will also as already mentioned give rise to compressive isostatic pressure, but it is only acting on an atomic level. Larger bundles lead the system away from an atomic level. But also looking at the classical theory, the hydrostatic pressure from the surrounding matrix is inversely proportional to the radius of curvature, i.e.,

$$\Delta p = 2\gamma/r, \tag{2}$$

where γ is the surface energy of the interface and r the radius. It is to be noted that the cohesive energy density and surface energy are closely related. Higher radial compressive stresses will cause frictional forces and can increase the interfacial shear strength and thus the sensitivity. However, we are working at an atomic size level, and the classical continuum theory will not describe the situation accurately, but it is reasonable to assume that the effect is qualitatively correct.

The bundle sizes can be estimated from Fig. 12 showing scanning electron microscope (SEM) pictures of the carbon nanotube right after the ultrasonic dispersion in the solvent and before adding the polymer or epoxy resin. The emulsion was filtrated through a gold coated membrane filter leaving behind the carbon nanotube on the filter. For the purified carbon material a dense network is seen. The dichlorocarbene-modified CNT seems to be better dispersed. In the 5M HNO_3- and especially the 10M HNO_3-modified SWCNT the bundles are generally smaller. The HNO_3-modification is known to help exfoliating the SWCNT bundles resulting in smaller bundles [7].

Due to the stronger oxidizing power of the 10M HNO_3 compared with 5M HNO_3, a better dispersion and higher degree of exfoliation is expected. For the octadecylamine-

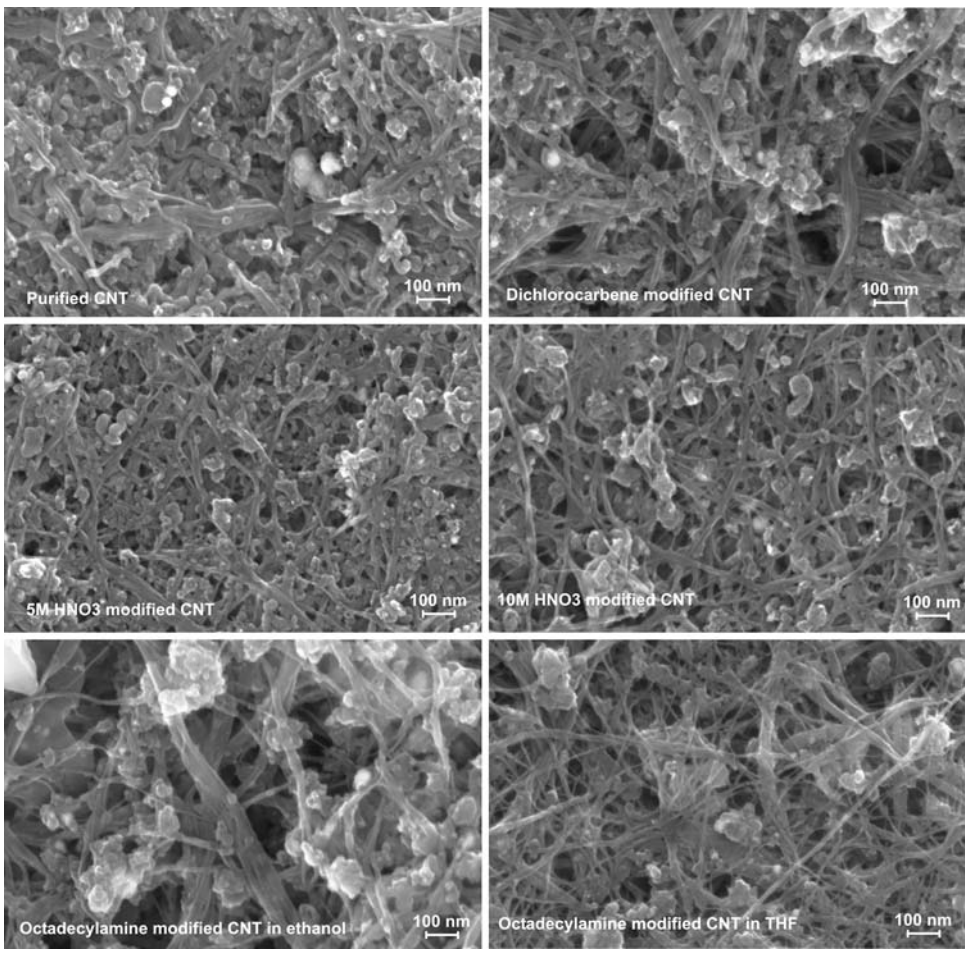

Fig. 12 SEM images of the modified or simply purified SWCNT after ultrasonical dispersion in ethanol or THF and filtrated through a gold-coated membrane filter

modified SWCNT, a clear distinction is seen between ethanol- and the THF-suspended samples. The octadecylamine-modified SWCNT are to some degree soluble in THF, whereas it was impossible to form any good suspension in ethanol. In ethanol, the bundles are thick and in THF the bundles are much finer.

The influence of the modification itself is somewhat unclear. Dichlorocarbene modification seems to give no improvement. Octadecylamine modification is beneficial when added to a PC matrix, but no improvement is seen in epoxy. In epoxy, the peak position at zero strain is low despite the good dispersion in THF. An explanation could be that the small bundles are unstable in epoxy and eventually after the evaporation of the solvent, the nanotubes re-assemble in larger bundles. For the HNO_3 modification, the increased interfacial shear strength can be explained by smaller bundle sizes caused by exfoliation.

Conclusion

The interfacial strength was evaluated by measuring the shift of the G′-band of the SWCNT. The most effective functionalization in order to enhance the interfacial strength was a simple treatment by HNO_3 yielding carboxylic acid groups on the walls of the nanotube. The effect was not as much a result of the functionalization itself but due to the fact that the HNO_3 treatment exfoliated the bundles decreasing the diameter of the bundles and thus increasing the interface area and also increasing the compressive forces on the bundles resulting in larger frictional forces. Dichlorocarbene modification seems to give no improvement in the interfacial strength. Octadecylamine modification seems to improve the interfacial strength for a PC-composite material but not for epoxy.

The position of the G-peak at zero strain seems to give an indication of the size of the bundles and thus could be used as an indication of the quality of the dispersion or rather the exfoliation of the carbon nanotube material in the matrix.

References

1. Wood JR, Frogley MD, Meurs ER, Prins AD, Peijs T, Dunstan DJ, Wagner HD (1999) J Phys Chem 103:10388
2. Wood JR, Zhao Q, Frogley MD, Meurs ER, Prins AD, Peijsa T, Dunstan DJ, Wagner HD (2000) Phys Rev B 62(11):7571
3. Zhao Q, Frogley MD, Wagner HD (2002) Compos Sci Technol 62:147
4. Hwang J, Gommans HH, Ugawa A, Tashiro H, Haggenmueller R, Winey KI, Fisher JE, Tanner DB, Rinzler AG (2000) Phys Rev B 62:13310
5. Frogley MD, Zhao Q, Wagner HD (2002) Phys Rev B 65:113413
6. Chen Y, Haddon RC, Fang S, Rao AM, Eklund PC, Lee WH, Dickey EC, Grulke EA, Pendergrass JC, Chavan A, Haley BE, Smalley RE (1998) J Mater Res 13(9):2423
7. Liu J, Rinzler AG, Dai H, Hafner JH, Bradley RK, Boul PJ, Lu A, Iverson T, Shelimov K, Huffmann CB, Rodriguez-Macias F, Shon Y, Lee TR, Colbert DT, Smalley RE (1998) Science 280(5367):1253
8. Chen J, Rao AM, Lyuksyutov S, Itkis ME, Hamon MA, Hu H, Cohn RW, Eklund PC, Colbert DT, Smalley RE, Haddon RC (2001) J Phys Chem B 105:2525
9. Nyquist RA (2001) Interpreting infrared, Raman, and nuclear magnetic resonance spectra. Academic Press, San Diego
10. Frogley MD, Ravich D, Wagner HD (2003) Compos Sci Technol 63:1647
11. Cronin SB, Swan AK, Ünlü MS, Goldberg BB, Dresselhaus MS, Tinkham M (2005) Phys Rev B 72:035425
12. Kannan P, Eichhorn SJ, Young RJ (2007) Nanotechnology 18:235707
13. Huang Y, Young RJ (1995) Composites 26:541
14. Cox HL (1952) Brit J Appl Phys 3:72
15. Lucas M, Young RJ (2007) Compos Sci Technol 67:840